AGU PUBLICATIONS

Geophysical Research Letters

RESEARCH LETTER

10.1002/2013GL059175

Special Section:
Early Results from the Van Allen Probes(Closed to new submissions Nov 1, 2013)

Key Points:
- An overview of the He ion abundance during the first 9 months of observations
- The appearance of a high energy, low L-shell He ion population
- How the injected He ions respond on daily timescales

Correspondence to:
A. Gerrard,
gerrard@njit.edu

Citation:
Gerrard, A., L. Lanzerotti, M. Gkioulidou, D. Mitchell, J. Manweiler, and J. Bortnik (2014), Quiet time observations of He ions in the inner magnetosphere as observed from the RBSPICE instrument aboard the Van Allen Probes mission, *Geophys. Res. Lett.*, *41*, doi:10.1002/2013GL059175.

Received 30 DEC 2013
Accepted 27 JAN 2014
Accepted article online 30 JAN 2014

Quiet time observations of He ions in the inner magnetosphere as observed from the RBSPICE instrument aboard the Van Allen Probes mission

Andrew Gerrard[1], Louis Lanzerotti[1], Matina Gkioulidou[2], Donald Mitchell[2], Jerry Manweiler[3], and Jacob Bortnik[4]

[1]Center for Solar-Terrestrial Research, New Jersey Institute of Technology, Newark, New Jersey, USA, [2]John Hopkins University-Applied Physics Laboratory, Laurel, Maryland, USA, [3]Fundamental Technologies, LLC, Lawrence, Kansas, USA [4]University of California at Los Angeles, California, USA

Abstract He ions contribute to Earth's ring current energy and species population density and are important in understanding ion transport and charge exchange processes in the inner magnetosphere. He ion flux measurements made by the Van Allen Probes Radiation Belt Storm Probes Ion Composition Experiment (RBSPICE) instrument are presented in this paper. Particular focus is centered on geomagnetically quiet intervals in late 2012 and 2013 that show the flux, L-shell, and energy (65 keV to 518 keV) morphology of ring current He ions between geomagnetic storm injection events. The overall He ion abundance during the first nine months of RBSPICE observations, the appearance of a persistent high energy, low L-shell He ion population, and the temporal evolution of this population all provide new insights into trapped ring current energy He ions. These data provide a unique resource that will be used to provide verifications of, and improvements to, models of He ion transport and loss in Earth's ring current region.

1. Introduction

Measurements from the Radiation Belt Storm Probes Ion Composition Experiment (RBSPICE) instruments on the Van Allan Probes spacecraft provide the opportunity to determine, over extended time and spatial intervals, the hydrogen, helium, and oxygen ion abundances at ring current energies in Earth's inner magnetosphere. The near-equatorial orbits of the Van Allen Probes [*Mauk et al.*, 2012] are particularly useful for the characterization of the fluxes of these ion species. Thus, RBSPICE was designed and implemented to provide information on the composition and dynamics of Earth's ring current during all levels of geomagnetic activity [*Mitchell et al.*, 2012]. Energy spectra and relative abundance measurements for trapped ions over various energy ranges and for the dominant ionic species (H, He, and O) have been reported by a number of investigators since early in the space age, including for example, *Krimigis* [1963], *Frank* [1967], *Smith and Hoffman* [1973], *Konradi et al.* [1973], *Ejiri et al.* [1980], *Williams* [1981], *Lundin et al.* [1980], *Gloeckler et al.* [1985], *Krimigis et al.* [1985], *Hamilton et al.* [1988], *Kistler et al.* [1989], *Roeder et al.* [1996], *Daglis et al.* [1999], *Fu et al.* [2001], *Ebihara et al.* [2002], *Greenspan and Hamilton* [2002], *Fu et al.* [2003], and *Dandouras et al.* [2009].

Of particular interest herein is the morphology of He ions during geomagnetic quiet times in the inner magnetosphere, which is important for providing contemporary baselines for magnetospheric species of trapped particles, for a better understanding of abundances in disturbed intervals, and for testing our understanding of ion source, loss, transport, and charge exchange mechanisms. The first quiet time He ion model was presented in *Spjeldvik and Fritz* [1978]. However, this study could not test the validity of the model with experimental data for He ions below 1 MeV. Later, quiet time Active Magnetospheric Particle Tracer Explorers (AMPTE)/CCE/charge-energy-mass (CHEM) He ion measurements across the 1–300 keV energy range were modeled by *Sheldon and Hamilton* [1993] and *Sheldon* [1994]. Of particular interest in these later studies was the overprediction of He ions at L-shells of ~4 and at energies >100 keV (which was also reproduced in model results of *Spjeldvik and Fritz* [1978]), which could not be satisfactorily explained and is still unresolved.

This paper reports near-equatorial He ion abundance measurements from the RBSPICE instrument during geomagnetically quiet intervals in late 2012 (following instrument commissioning) and 2013. The data presented herein, all from Van Allan Probes spacecraft B, show the abundance, L-shell, and energy morphology

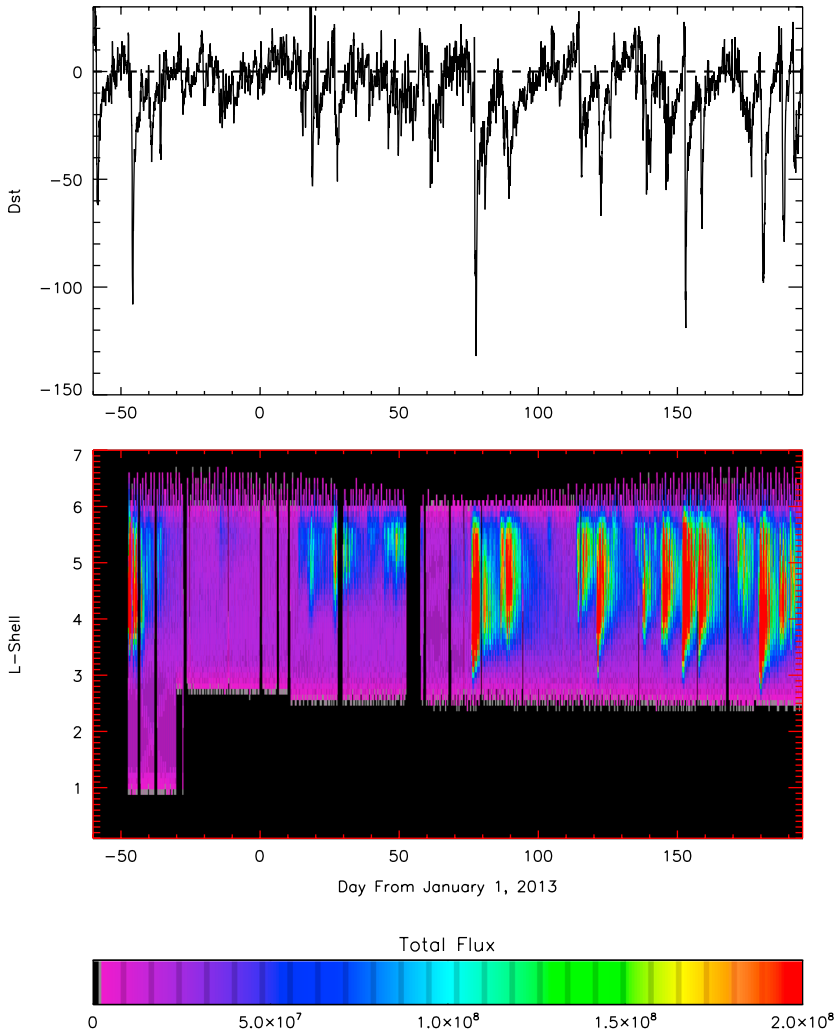

Figure 1. (top) Hourly *Dst* values as reported from the World Data Center (WDC) for Geomagnetism, Kyoto, Japan. Time is measured in days from 1 January 2013. (bottom) He ion flux (particles/(second per square centimeter)), between the 65 keV and 518 keV energy range, as measured by the RBSPICE instrument aboard the Van Allan Probes spacecraft B, binned into 30 min, 0.1 L-shell realizations. L here is determined by a dipole L model. The measurements below L∼2.5 early in the mission demonstrate the original data window of RBSPICE, which was subsequently reduced due to instrument constraints.

of He ions during geomagnetic quiet times. Of unique interest is the appearance of He ions at energies above ∼100 keV and at L∼4, which were predicted in previous models. Furthermore, we note that this particular population seems well suited to testing He ion transport and loss mechanisms due to its temporal and spatial variability.

2. Observations

The He ion abundances reported are from the time of flight versus total energy (TOFxE) instrument feature [*Mitchell et al.*, 2012] and thus cover the ∼65 keV to ∼518 keV energy range. The RBSPICE instrument was not designed to differentiate between He ion charge states (i.e., He^{+} and He^{+2}). However, the data focused on herein corresponds to geomagnetic quiet times and are therefore dominated by He^{+} (i.e., solar wind injected He^{+2} should be quite low during these periods). The fluxes are integrated over all pitch angles as measured by the six "telescopes" (i.e., independent fields of view) of the RBSPICE instrument. All measurements shown here are well above the instrument noise floor and are statistically significant, as based on Poisson counting statistics.

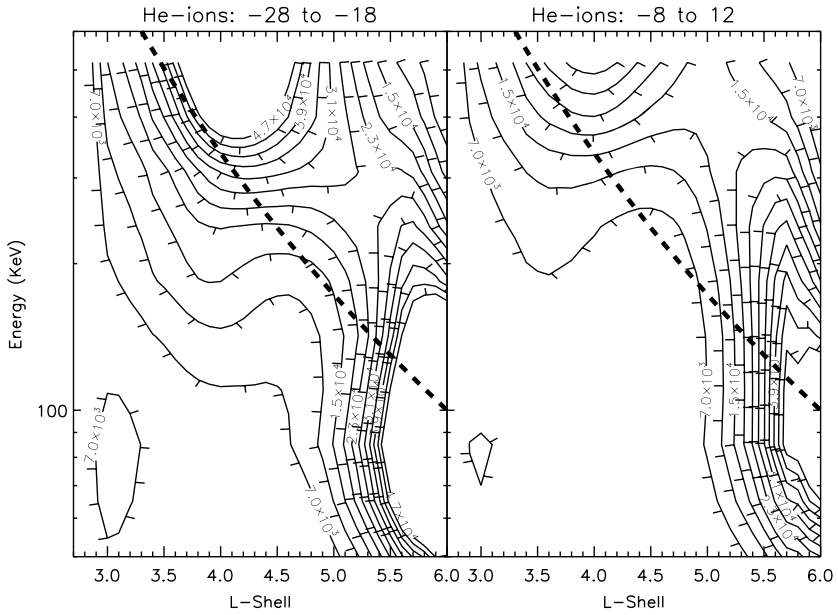

Figure 2. Two, sample, quiet time averages of He ion flux (particles/(second per square centimeter per kiloelectron volt)) displayed in an energy/L-shell distribution. L here is determined by a dipole L model. Dashed black lines represent the first adiabatic energy trace for a 100 keV particle located at L=6.

Figure 1 (bottom) shows the total (i.e., omnidirectional and energy integrated) He ion fluxes (particles/(second per square centimeter)) in the measured energy range as a function of dipole L-shell beginning shortly after instrument commissioning (1 November 2012) and running to day 200 (19 July) 2013. The data have been placed in 30 min and 0.1 L-shell data bins, thus smearing high flux values associated with injections at higher L-shells at spacecraft apogee. The hourly *Dst* index for the same time interval is shown in

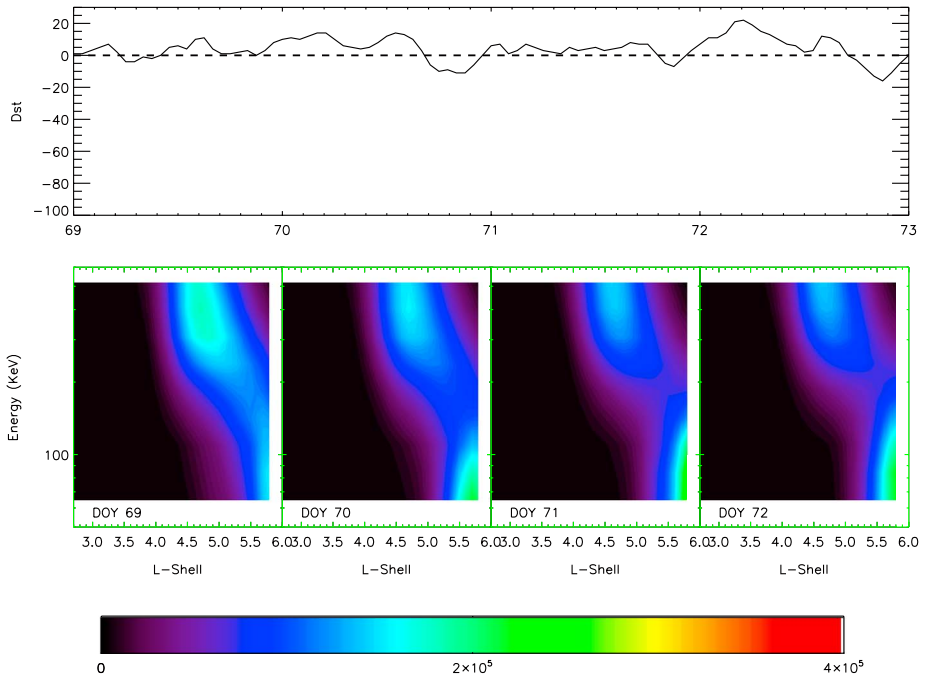

Figure 3. (top) Hourly *Dst* values as reported from the WDC for Geomagnetism, Kyoto, Japan. Time is measured in days from 1 January 2013. (bottom) Sequence of 1 day averages of He ion flux (particles/(second per square centimeter per kiloelectron volt)) displayed in an energy/L-shell distribution between 2013 day of year (DOY) 69 and 72. L here is determined by a dipole L model.

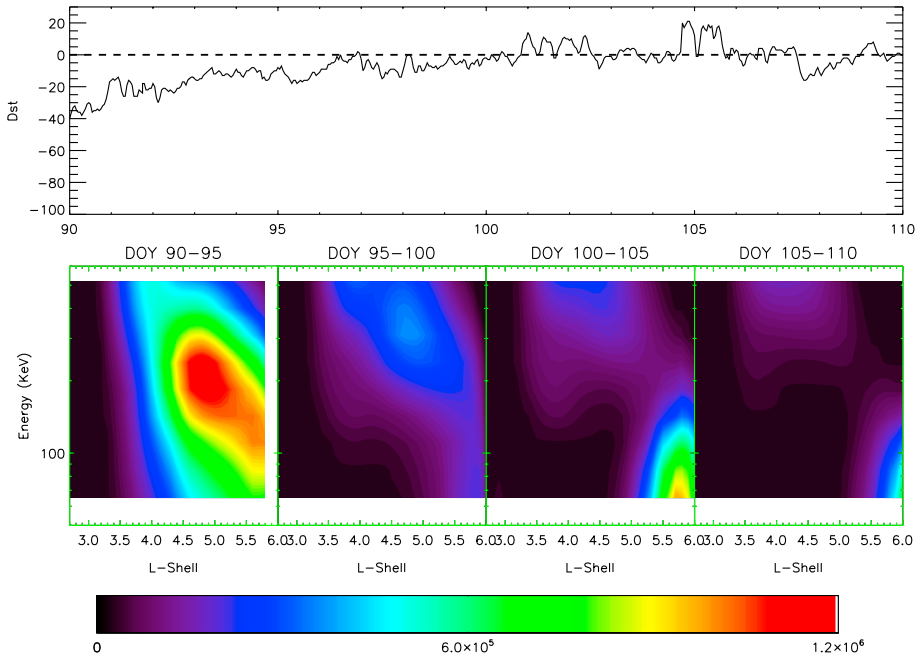

Figure 4. (top) Hourly *Dst* values as reported from the WDC for Geomagnetism, Kyoto, Japan. Time is measured in days from 1 January 2013. (bottom) Sequence of 5 day averages of He ion flux (particles/(second per centimeter per kiloelectron volt)) displayed in an energy/L-shell distribution between 2013 DOY 90 and 110. L here is determined by a dipole L model.

Figure 1 (top). Data gaps are the result of changes in instrument configuration and in calibration upgrades of in-flight and processing software. Enhancements of the He ion abundances, often lasting for several days, are clearly seen to occur at the times of geomagnetic disturbances as indicated by the low values of the *Dst* index.

Of particular interest are two intervals of extended geomagnetic quiet time in late 2012 and early 2013: days −28 to −18 (i.e., day 339 to 349, 2012) and days −8 to 12 (i.e., day 359, 2012 to day 12, 2013). Days −17 to −9 (i.e., day 350 to 358, 2012) are not included in this period due to the short, intense He ion enhancement observed between L∼5 and 6 (and also seen in the *Dst* index). Shown in Figure 2 are contour plots of the He ion fluxes (particles/(second per square centimeter per kiloelectron volt)) as a function of energy and dipole L-shell for these two periods. Two distinct populations of He ions are evident, specifically an enhanced concentration at higher energies (∼400 keV and higher) at L∼4.0, and another enhanced concentration at lower energies (∼80 keV) at L∼6. A "saddle point" between the He ions groups is observed around L∼5.0 and between ∼300 keV and ∼400 keV. The He ion population varies somewhat in L-shell and energy range between the two data intervals. The abundance contours trend toward and follow the dashed black lines, which represent a sample first adiabatic energy trace for a 100 keV particle located at L=6. This structure of the He ion fluxes suggests inward radial motion (and energization) of the particle populations [e.g., *Schulz and Lanzerotti*, 1974], which were likely initially injected into the higher L-shell region at lower energies.

While Figure 2 depicts the quiet time, "steady state" structure of the ring current He ions, Figure 3 demonstrates the evolution of "quiet time" He ions on a daily timescale. These quiet time data are from a 4 day interval days 69–72, just prior to a large geomagnetic storm on day 76 (17 March). On day 69, the He ion fluxes are enhanced in the same two general regions as in Figure 2. However, the high-energy population is located at a higher L-shell. Over the course of the following 3 days, the higher-energy He ion population decays in flux, while the lower energy population flux increases. The saddle point between the two regions remains relatively stationary.

Evolution of the "quiet time" He ion morphology is even more evident just after an injection event, as shown between days 90 and 110 in Figure 4. Each panel consists of a 5 day average of the He ion fluxes as a function of energy and dipole L-shell. The first 5 day interval (days 90–95) shows a large concentration of He ions at moderate L values following the geomagnetic storm event (i.e., as seen in the *Dst* index). He ion fluxes

were highly concentrated in a broad energy and spatial range of ~70 keV to ~300 keV and L~4.0 and L~5.8, respectively. The day 95–100 interval shows evidence of radial transport via diffusion of the He ion fluxes to higher energies and lower L values. In the day 100–105 interval, the lower energy He ion fluxes suddenly increase in magnitude (at L~5.7), while the lower L value, higher-energy fluxes decrease further in intensity. It is this time interval that the two He ion regions can be best differentiated and a clear saddle point identified. Finally, in the interval day 105–110, prior to another geomagnetic storm, the intensity of the higher L-shell, lower energy fluxes appear to move to L~6, and the lower L-shell fluxes continue to decrease.

3. Discussions and Conclusions

As the data presentations show, the RBSPICE instrument provides information on the nonstorm time, ring current energy range, He ion fluxes in Earths magnetosphere. The He ion abundance values of Figure 1 compare well to values reported in prior literature (i.e., about 1/100 of the measured proton flux; work in progress). Figures 2, 3, and 4 show two He ion populations, one around ~400 keV (and higher) at L~4.0 and another around ~80 keV at L~6 that are seen to persist throughout quiet intervals.

The He ion distributions shown in Figure 2 agree (qualitatively) well with the steady state modeling results of *Spjeldvik and Fritz* [1978], although that work seems to have overestimated the low L-shell, low-energy He ion population. This is likely due to the relatively large flux of He^{+2} used in that study as a boundary condition set at L= 7, which then converted to He^{+} via charge exchange mechanisms. The saddle point observed in Figure 2, referred to as a "hole" in *Spjeldvik and Fritz* [1978], is also well resolved both in data and model. *Spjeldvik and Fritz* [1978] argue that this saddle point is a consequence of a complex balance between ion transport, loss, and charge exchange. The two distinct regions of He ions and the saddle point observed in Figure 2 is also observed in data published from CRRES/magnetospheric ion composition spectrometer (MICS) He^{+} (but not He^{+2}) data [*Fu et al.*, 2001, 2003]. However, their existence is not commented on.

The high-energy, low L-shell region and saddle point also appear in the models of *Sheldon and Hamilton* [1993] and *Sheldon* [1994]. However, as discussed at length in *Sheldon* [1994], the AMPTE/CCE/CHEM He ion measurements did not show such a high-energy, low L-shell population, and this led to a large discrepancy between subsequent model and data comparisons. It is currently unclear why the AMPTE/CCE/CHEM He ion measurements do not show this population, and one speculates if the issue was associated with counting statistics. The data presented herein, however, clearly show this population and verify these earlier model efforts and CRRES/MICS data. For completeness, this population is also clearly present when we transform the data presented in Figures 2, 3, and 4 into phase space distributions as functions of L-shell and magnetic moment to directly compare to the AMPTE data presented in*Sheldon and Hamilton* [1993] and *Sheldon* [1994].

The He ion energy/L-shell structure of Figure 2 and the temporal/spatial evolution shown in Figures 3 and 4 beckons a revisit of the modeling efforts of *Sheldon and Hamilton* [1993] and *Sheldon* [1994], where a Fokker-Planck equation, utilizing updated parameterizations, can be used to study the evolution of He ions in Earth's ring current. Such an effort could provide needed closure on the steady state and slow temporal evolution of He ions in Earth's ring current.

These Van Allen Probe results show that trapped He ions exist for extended intervals in the magnetosphere and with important spatial distributions. Such ions form a dynamic component of the quiet time radiation belts, particularly at the higher L values. The origins of these trapped He ion particles is a subject long debated in magnetosphere studies [e.g., *Daglis et al.*, 1999] and is not the subject of this report. However, if substorm injections events are frequent enough such that He ion loss times exceed the substorm frequency intervals, then these higher L-shell He ions can form a source contributor of ring current ions. Future studies will examine extended intervals of geomagnetic quiet in order to understand further the persistence and lifetimes of high L-shell trapped He ions in Earth's magnetosphere.

Acknowledgments

The authors thank team discussions with the larger RBSPICE and Van Allan Probes teams. The RBSPICE instrument was supported by JHU/APL subcontract 937836 to the New Jersey Institute of Technology under NASA Prime contract NAS5-01072. The *Dst* hourly data came from the WDC for Geomagnetism, Kyoto, Japan. Two anonymous reviewers provided great help in the evaluation and improvement of this paper.

The Editor thanks two anonymous reviewers for their assistance in evaluating this paper.

References

Daglis, I. A., R. Thorne, W. Baumjohann, and S. Orsini (1999), The terrestrial ring current: Origin, formation, and decay, *Rev. Geophys.*, *37*(4), 407–438, doi:10.1029/1999RG900009.

Dandouras, I., J. Cao, and C. Vallat (2009), Energetic ion dynamics of the inner magnetosphere revealed in coordinated Cluster-Double Star observations, *J. Geophys. Res.*, *114*, A01S90, doi:10.1029/2007JA0122757.

Ebihara, Y., M. Ejiri, H. Nilsson, I. Sandahl, A. Milillo, M. Grande, J. F. Fennell, and J. L. Roeder (2002), Statistical distribution of the storm-time proton ring current: Polar measurements, *Geophys. Res. Lett.*, *29*(20), 1969, doi:10.1029/2002GL015430.

Ejiri, M., R. A. Hoffman, and P. H. Smith (1980), Energetic particle penetration into the inner magnetosphere, *J. Geophys. Res.*, *85*, 653–663, doi:10.1029/JA085A02p00653.

Frank, L. A. (1967), On the geomagnetic ring current during geomagnetic storms, *J. Geophys. Res.*, *72*, 3753–3767, doi:10.1029/JZ072i015p03753.

Fu, S. Y., Q. G. Zong, B. Wilken, and Z. Y. Pu (2001), Temporal and spatial variation of ion composition in the ring current, *Space Sci. Rev.*, *95*, 539–554.

Fu, S., Q. Zong, Z. Pu, and W. Liu (2003), Effects of geomagnetic and solar activities on the composition and position of the ring current ion, *Chinese J. Geophys.*, *46*(6), 1041–1049.

Gloeckler, G., F. M. Ipavich, B. Wilken, W. Stuedemann, and D. Hovestadt (1985), First composition measurement of the bulk of the storm-time ring current (1 to 300 KeV/e) with AMPTE-CCE, *Geophys. Res. Lett.*, *12*, 325–328, doi:10.1029/GL012i005p00325.

Greenspan, M. E., and D. C. Hamilton (2002), Relative contributions of H^+ and O^+ to the ring current energy near magnetic storm maximum, *J. Geophys. Res.*, *107*, 1043, doi:10.1029/2001JA000155.

Hamilton, D. C., G. Gloeckler, F. M. Ipavich, W. Studemann, B. Wilken, and G. Kremser (1988), Ring current development during the great geomagnetic storm of February 1986, *J. Geophys. Res.*, *93*, 14,343–14,355, doi:10.1029/JA093iA12p14343.

Kistler, L. M., F. M. Ipavich, D. C. Hamilton, G. Gloeckler, B. Wilken, G. Kremser, and W. Studemann (1989), Energy-spectra of the major ion species in the ring current during geomagnetic storms, *J. Geophys. Res.*, *94*, 3579–3599, doi:10.1029/JA094iA04p03579.

Konradi, A., D. J. Williams, and T. A. Fritz (1973), Energy-spectra of the major ion species in the ring current during geomagnetic storms, *J. Geophys. Res.*, *78*, 4739–4744, doi:10.1029/JA078i022p04739.

Krimigis, S. M. (1963), Solar protons and their geophysical effects, *Proc. Iowa Academy of Sci.*, *70*, 393–402.

Krimigis, S. M., G. Gloeckler, R. W. McEntire, T. A. Potemra, F. L. Scarf, and E. G. Shelley (1985), Magnetic storm of September 4, 1984: A synthesis of ring current spectra and energy densities measured with AMPTE/CCE, *Geophys. Res. Lett.*, *12*, 329–332, doi:1029/GL012i005p00329.

Lundin, R., L. R. Lyons, and N. Pissarenko (1980), Observations of the ring current composition at $L < 4$, *Geophys. Res. Lett.*, *7*, 425–428, doi:10.1029/GL007i006p00425.

Mauk, B. H., N. J. Fox, S. G. Kanekal, R. L. Kessel, D. G. Sibeck, and A. Ukhorskiy (2012), Science objectives and rationale for the radiation belt storm probes mission, *Space Sci. Rev.*, *179*, 3–27, doi:10.1007/s11214-012-9908-y.

Mitchell, D., et al. (2012), Radiation Belt Storm Probes Ion Composition Experiment (RBSPICE), *Space Sci. Rev.*, *179*, 263–308, doi:10.1007/s11214-013-9965-x.

Roeder, J. L., J. F. Fennell, M. W. Chen, M. Schulz, M. Grande, and S. Livi (1996), CRRES observations of the composition of the ring-current ion populations, *Adv. Space Res.*, *17*(10), 17–24, doi:10.1016/0273-1177(95)00689-C.

Sheldon, R. B. (1994), Ion transport and loss in the Earth's quiet ring current. 2: Diffusion and magnetosphere-ionosphere coupling, *J. Geophys. Res.*, *99*, 5705–5720, doi:10.1029/93JA02769.

Sheldon, R. B., and D. C. Hamilton (1993), Ion transport and loss in the Earth's quiet ring current. I - Data and standard model, *J. Geophys. Res.*, *98*, 13,491–13,508, doi:10.1029/92JA02869.

Smith, P. H., and R. A. Hoffman (1973), Ring current particle distributions during the magnetic storms of December 16–18, 1971, *J. Geophys. Res.*, *78*, 4731–4737, doi:10.1029/JA078i022p12079.

Spjeldvik, W. N., and T. A. Fritz (1978), Energetic ionized helium in the quiet time radiation belts—Theory and comparison with observation, *J. Geophys. Res.*, *83*, 654–662, doi:10.1029/JA083iA02p00654.

Schulz, M., and L. J. Lanzerotti (1974), *Particle Diffusion in the Radiation Belts, Physics and Chemistry in Space*, Springer, Berlin.

Williams, D. J. (1981), Ring current composition and sources: An update, *Planet. Space Sci.*, *29*, 1195–1203, doi:10.1016/0032-0633(81)90124-0.